engineering proceedings

MDPI

Proceeding Paper

On the Sensitivity of the Potential Evapotranspiration of Egypt to Different Dynamical Downscaling Options and Boundary Layer Schemes Using a High-Resolution Regional Climate Model (RegCM4) †

Samy Ashraf Anwar [1,*] and Ankur Srivastava [2,*]

[1] Egyptian Meteorological Authority, Qobry EL-Kobba, Cairo P.O. Box 11784, Egypt
[2] Faculty of Science, University of Technology Sydney, Sydney, Australia
* Correspondence: ratebsamy@yahoo.com (S.A.A.); ankursrivastava117@gmail.com (A.S.)
† Presented at the 4th International Electronic Conference on Applied Sciences, 27 October–10 November 2023; Available online: https://asec2023.sciforum.net/.

Abstract: Providing accurate information of potential evapotranspiration (PET) is mandatory for arid regions (such as Egypt) for assessing the crop water requirements. Such precision is limited by the dynamical downscaling options and the physical settings used in regional climate models (like RegCM4). To address these issues, four simulations were run as part of the current study. The first two simulations take direct (DIR) and one-way nesting (NEST) into account, while the other two use two boundary layer techniques (HOLTSLAG; HOLT) and (University of Washington; UW). All simulations were driven by ERA-Interim reanalysis of 1.5 degrees. The simulated PET was evaluated with respect of high-resolution reanalysis gridded derived product of the ERA5-Land (hereafter ERA5). The findings revealed that while there is no discernible difference between DIR and NEST in terms of the global incident solar radiation (RSDS). Also, NEST has a higher mean air temperature (TMP) than DIR. Additionally, UW has a lower TMP than HOLT, but switching between HOLT and UW did not impose a considerable impact on the simulated RSDS. Concerning PET, it is affected neither by switching between DIR and NEST or between HOLT and UW. Such results suggest that the RSDS is the main driver in controlling the PET variability followed by TMP. Therefore, using the DIR downscaling option and HOLT/UW boundary layer scheme throughout the 1980–2010, as recommended by the World Meteorological Organization, the RegCM4 model can be used to develop a regional PET map of Egypt.

Keywords: DIR; NEST; HOLT; regional climate model; PET

Citation: Anwar, S.A.; Srivastava, A. On the Sensitivity of the Potential Evapotranspiration of Egypt to Different Dynamical Downscaling Options and Boundary Layer Schemes Using a High-Resolution Regional Climate Model (RegCM4). *Eng. Proc.* **2023**, *52*, x. https://doi.org/10.3390/xxxxx

Academic Editor(s): Name

Published: date

1. Introduction

The Fourth Assessment Report of the Intergovernmental Panel on Climate Change (IPCC; [1]) reported that the Middle East and Northern Africa (MENA; as a hot-spot water scarce region) shows a high rate of water need (represented by potential evapotranspiration; PET) as a result of mean air temperature increase particularly under the Representative Concentration Pathway 8.5 (RCP8.5). Although the Penman-Monteith equation (PM; [2]) has been recommended to compute the PET because it is based on physical principles governing the physical exchange of water and energy between the surface and atmosphere, it requires many atmospheric variables (most of them are calculated empirically leading to a large increase of the uncertainty of the computed PET as reported by [3,4]). Instead, the Hargreaves–Samani equation (HS; [5]) was used to compute the PET. The HS equation has several advantages such as: it is recommended directly after the PM [3,4,6],

also it provides an easy way to track the future projected PET changes (as a function of mean air temperature) under different future scenarios.

Construction of a regional PET map (either in the present climate or under different future scenarios) can be done by using high−resolution regional climate models (RCMs such as RegCM4; [7]). Additionally, accurate estimation of the atmospheric variables (especially those involved in computing the PET) can be ensured by investigating different options of the dynamical downscaling or various combinations of the physical schemes (e.g., boundary layer). For instance, the authors of [8] reported that high-resolution RCMs and an improved physical parameterization can ensure a very high capability to reproduce the large scale atmospheric circulations. Also, the authors of [9] made various experiments to constrain the mean air temperature and total surface precipitation with respect to various reanalysis products using the RegCM4 model. They reported that direct downscaling to high-resolution ensures a better performance than adopting a one-way nesting technique.

Over Egypt, the author or [10] reported that direct downscaling outperforms the one-way nesting concerning the daily mean air temperature using the RegCM4. Additionally, the authors of [11] examined the role of boundary layer schemes in constraining the daily mean air temperature using the RegCM4. They reported that the University of Washington scheme (UW; [12]) is better in simulating the mean air temperature than the HOLTSLAG (HOLT; [13]) with respect to ERA5 reanalysis product. Additionally, the authors of [10 and 11] observed that the global incident solar radiation not affected neither by the options of the dynamical downscaling (direct or one-way nesting) nor by the boundary layer schemes (HOLT or UW). The authors of [4] examined the role of lateral boundary condition (driving the RegCM4 model) and the added value of the calibrated HS equation in simulating the ERA5 product. However, the influence of different options of the dynamical downscaling or boundary layer schemes on the simulated PET of Egypt was not examined in this study. Therefore, the target of the present study is to:

1. Examine the influence of dynamical downscaling options (direct versus one-way nesting) and boundary layer schemes (HOLT versus UW) on the simulated PET in comparison with ERA5 reanalysis product as the ground truth of observations of the PET.
2. Examine the dependence of the simulated PET on the global incident solar radiation and daily mean air temperature (as inputs of the HS equation) by constructing a regional map of the Pearson correlation coefficient in each case. The significant correlation was calculated using student *t*-test of alpha equals to 5%.
3. Investigating the performance of the RegCM4 concerning the climatological annual cycle of the PET with respect to ERA5 for locations defined by [3].

Section 2 describes the study area and experiment design; Section 3 shows the results of the study. Section 4 provides the discussion and conclusion.

2. Materials and Methods

2.1. Study Area

Egypt (as an important country in the MENA region) is bounded by the Mediterranean Sea from the north and the Red Sea from the east. From a climatic point of view, Egypt is categorized as semi-arid, with minimal precipitation. Concerning the wind regime, Egypt is characterized by a particular regime along the Red Sea and Mediterranean shores. According to the Köppen climate classification, Egypt is classified as a desert climate (BWh Egypt receives between 20 and 200 mm of annual average precipitation along the Mediterranean coast. Concerning relative humidity, the maximum and annual values vary with the region of study. For instance, Cairo has minimum values during spring (around 48%) and maximum values in summer (around 70%). In addition, Egypt is characterized by heatwaves during the spring and summer seasons (intense in Upper Egypt and moderate in the Northern Coast).

Concerning the coast of the Mediterranean Sea, the dominant wind direction is northwest, which can explain the moderate temperature along the Mediterranean coast. However, the situation is different in the central and the southern sectors because nighttime temperatures are very hot, especially in the summer, when average high temperatures can exceed 40 °C, as in Aswan, Luxor, Asyut or Sohag. Additionally, the high-elevation topography (e.g., Saint Catherine Mountains) plays an important role in cooling the nighttime temperature [14].

2.2. Experiment Design

In the present study, we used the fourth generation of the RegCM regional climate model (RegCM4; [7]). The reader can find details of the RegCM4 in [4,6,7,15]. Concerning PET, the RegCM4 has been used to compute the PET in different regions such as Egypt [3,4], Bulgaria [6] and Tropical Africa [15]. To address the influence of different options of the dynamical downscaling and boundary layer schemes on the simulated PET, four experiments were conducted over the period 1997–2017. The first year was considered as a spin-up to initialize the RegCM4 model with an equilibrium state of the atmosphere as recommended by [15,16], so the actual analysis starts at 1998 and ends at 2017. In all simulations, the RegCM4 was downscaled by the ERA-Interim reanalysis of 1.5 degrees (EIN15; [17]). In the present study, the RegCM4's domain was customized with 25 km horizontal resolution with 60 grid points in both zonal and meridional directions centered at latitude 27° and longitude 30°. The RegCM4 was downscaled in all simulations by the EIN15 to provide the lateral boundary condition and sea surface temperature. Figure 1 shows the surface elevation of Egypt (in meters) including the locations reported in [3].

To serve the purpose of the present study, the four simulations were grouped to two cases. The first case considers the dynamical downscaling options: direct (DIR) and one-way nesting (NEST) following [10]. On the other hand, the second case manipulates the boundary layer scheme: HOLT and UW following [11]. In the four simulations, the PET was calculated using a calibrated version of the HS equation following [4]. In each case, the simulated PET was evaluated with respect to the derived ERA5-land reanalysis product [18]. In addition, the significant difference between the two simulations (of each case) was calculated using student *t*-test with alpha equals 5%. Figure S1 shows a methodological flowchart summarizing the steps of the present study. Please note that the simulated PET was calculated using a calibrated version of the HS equation following [4] in the four simulations. The calibrated HS equation is written as:

$$\boldsymbol{PET_{HS} = 0.0105 \times RSDS \times (TMP + 17.8)} \quad (1)$$

where RSDS is the global incident solar radiation (expressed in mm day^{-1} to match the PET unit; [2]) and TMP is the 2 m mean air temperature (in °C).

2.3. Validation Data

The authors of [4] reported long-term records of station PET data may not be available either spatially or temporally. However, a new high-resolution gridded PET reanalysis product (hPET; [18]) was developed. This product computes the PET using the PM equation and it retrieved the meteorological variables (involved in computing the PET) from ERA5-land product [19]. Originally, the hPET product is available in 0.1 degrees for duration of 40 years (1981–2021) in hourly time scale as well as daily sum.

According to [18], hPET shows a good consistency with available global PET products particularly Climate Research Unit (CRU; [20]). Besides, hPET product can be used in various topics such as ecohydrology, and drought propagation. Additional advantages of the hPET can be found in [18]. Recently, hPET was used to assess the RegCM4 model performance concerning the original and the calibrated version of the HS equation [4]. For the purpose of the present study, all products were bilinearly interpolated on the RegCM4 curvilinear grid following [10,15]. For evaluation of the RegCM4 on a point scale, all

locations reported in [3] were considered except for Port-Said and Marsa-Matruh because ERA5 gives missing records in these locations.

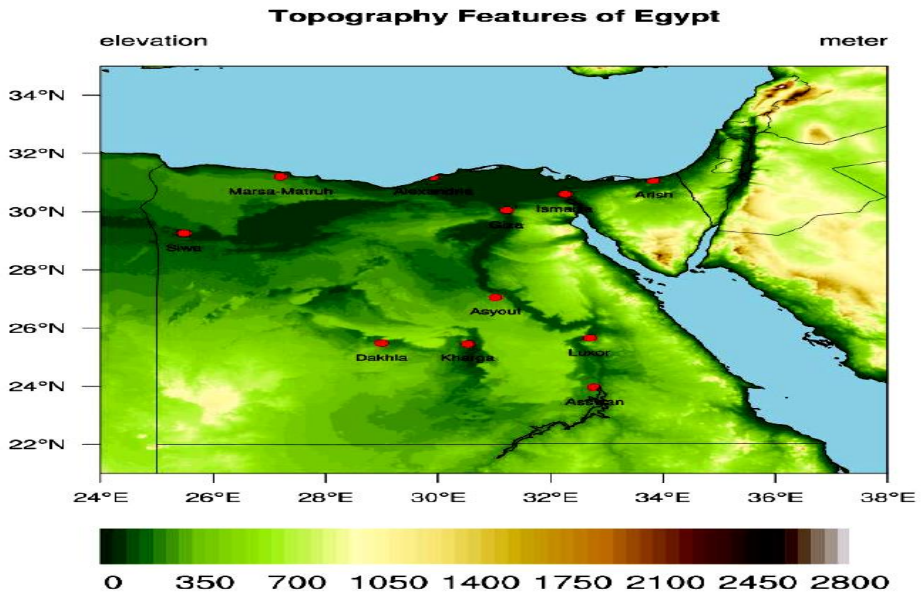

Figure 1. The figure shows surface elevation of Egypt (in meters). The red dots indicate the location of stations reported in [3] except of Port-Said where the hPET shows missed data.

3. Results

The authors of [4] reported that calibrating the coefficient of the global incident solar radiation (RSDS) is more efficient than calibrating the coefficient of the daily mean air temperature (TMP). Because the RSDS and TMP are inputs of the HS equation [4,6], it is important to investigate the influence of different options of the dynamical downscaling and boundary layer parameterization on the simulated RSDS and TMP to explain the observed changes of the simulated PET in each case. The author of [10] reported that dynamical downscaling (either DIR or NEST) shows insignificant impact on the simulated RSDS in all seasons.

Additionally, switching between DIR and NEST has a considerable impact on the simulated TMP through changes of the ground temperature and sensible heat flux particularly in the autumn season as NEST amplifies the positive bias compared to the DIR. Concerning the boundary layer parameterization, the authors of [11] observed that the UW has a lower TMP than the HOLT in all seasons particularly in the spring and winter seasons. Additionally, switching between HOLT and UW does not affect the simulated RSDS in all seasons.

3.1. Seasonal Climatology

3.1.1. Influence of Dynamical Downscaling Options on PET

Figure 2 explores the influence of dynamical downscaling options (DIR and NEST) on the simulated PET with respect to ERA5 reanalysis product as well as the difference between NEST and DIR. In general, it can be noted (from Figure 1) that the RegCM4 is able to reproduce the spatial pattern of the simulated PET with respect to ERA5 as the PET shows minimum values in the winter season (December-January-February ; DJF; Figure 2s–u) followed by the spring (March-April-May; MAM; Figure 2a–c) then summer (June-July-August; JJA; Figure 2g–l) and finally autumn (September-October-November; SON; Figure 2m–o). Additionally, both DIR and NEST shows a negative bias of the PET of 1–2 mm day^{-1} in the MAM and JJA seasons (Figure 2d,e,j,k). While in the SON seasons, both simulations show a positive bias of 1–2.5 mm day^{-1}. Finally in the DJF season, the RegCM4

bias is minimized (compared to the other seasons) because the bias equals approximately +0.5 mm day^{-1} (Figure 2v,w). Qualitatively, there is no difference between the two simulations in all seasons (see Figure 2f,l,r,x).

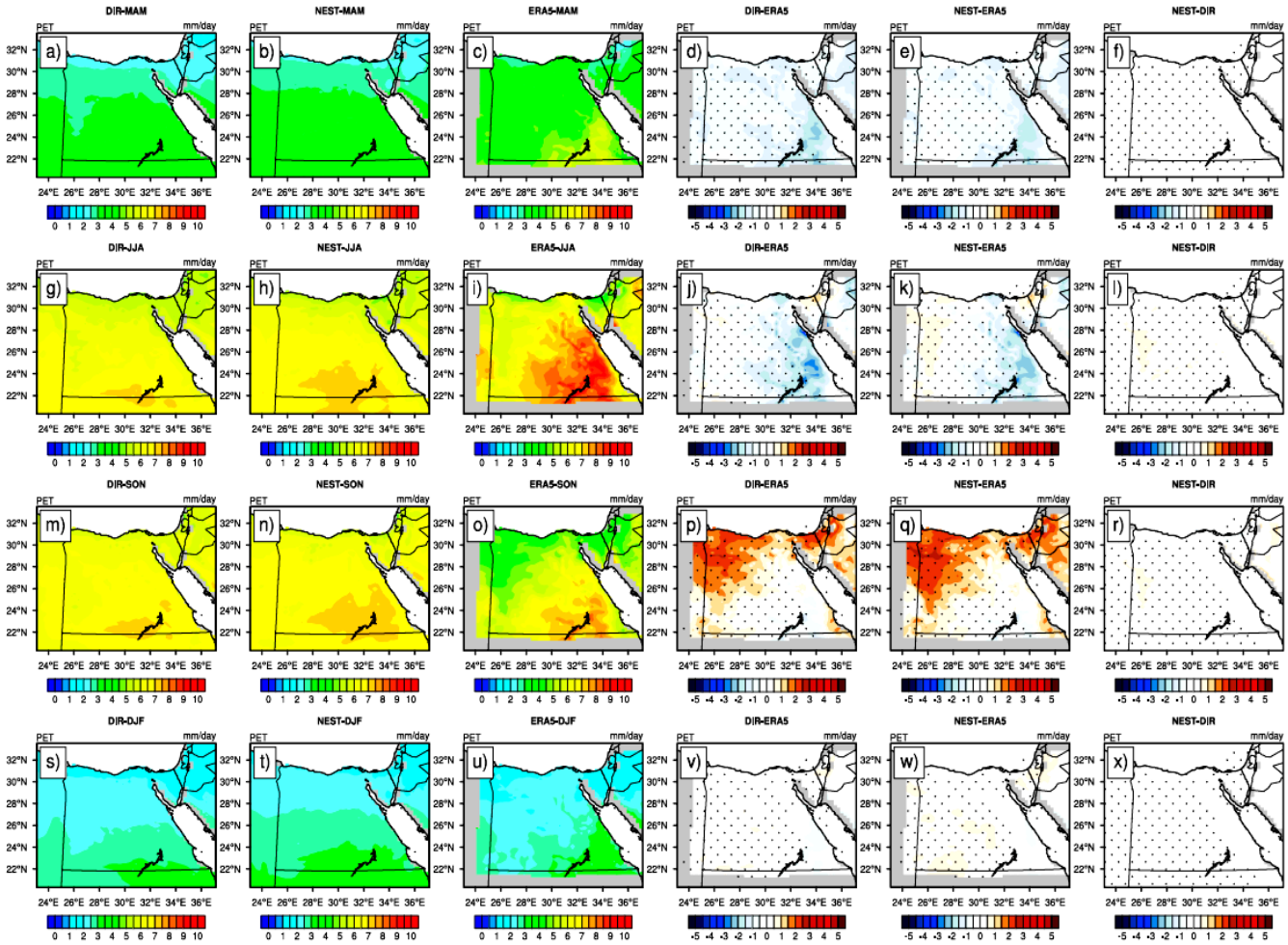

Figure 2. The figure shows the potential evapotranspiration over the period 1998–2017 (PET; in mm day^{-1}) for: MAM season in the first row (**a**–**f**); JJA in the second (**g**–**l**); SON in the third (**m**–**r**); and DJF in the fourth (**s**–**x**). For each row, DIR is on the left, followed by NEST; ERA5 is the third from left, DIR minus ERA5, NEST minus ERA5 and the difference between NEST and DIR. Significant difference/bias is indicated in black dots using student *t*-test with alpha equals to 5%.

3.1.2. Influence of Boundary Layer Schemes on PET

Figure 3 shows the simulated PET (by the HOLT and UW boundary layer schemes) in comparison with the ERA5 as well as the difference between the HOLT and UW. Like Figure 1, the RegCM4 successfully captures the spatial pattern of the PET with respect to ERA5 product in all seasons (Figure 3a–c,g–i,m–o,s–u). Also, the RegCM4 bias is similar to the one noted in the case of the dynamical downscaling in all seasons (Figure 3d,e,j,k,p,q,v,w). Lastly, there is no considerable difference between the two simulations in all seasons (see Figure 3f,l,r,x).

It can be noticed (From Figures 2 and 3) that the simulated PET is sensitive neither to the option of the dynamical downscaling (DIR/NEST) nor the boundary layer parameterization (HOLT/UW) despite of the noted changes of the TMP in both cases as reported by [10,11]. Therefore, it can be reported that the simulated PET is not affected (in both cases) because the RSDS is affected neither by the dynamical downscaling options nor the

boundary layer parameterization. Such behavior suggests that the RSDS is the main driver of controlling the PET; which will be further discussed in Section 3.2.

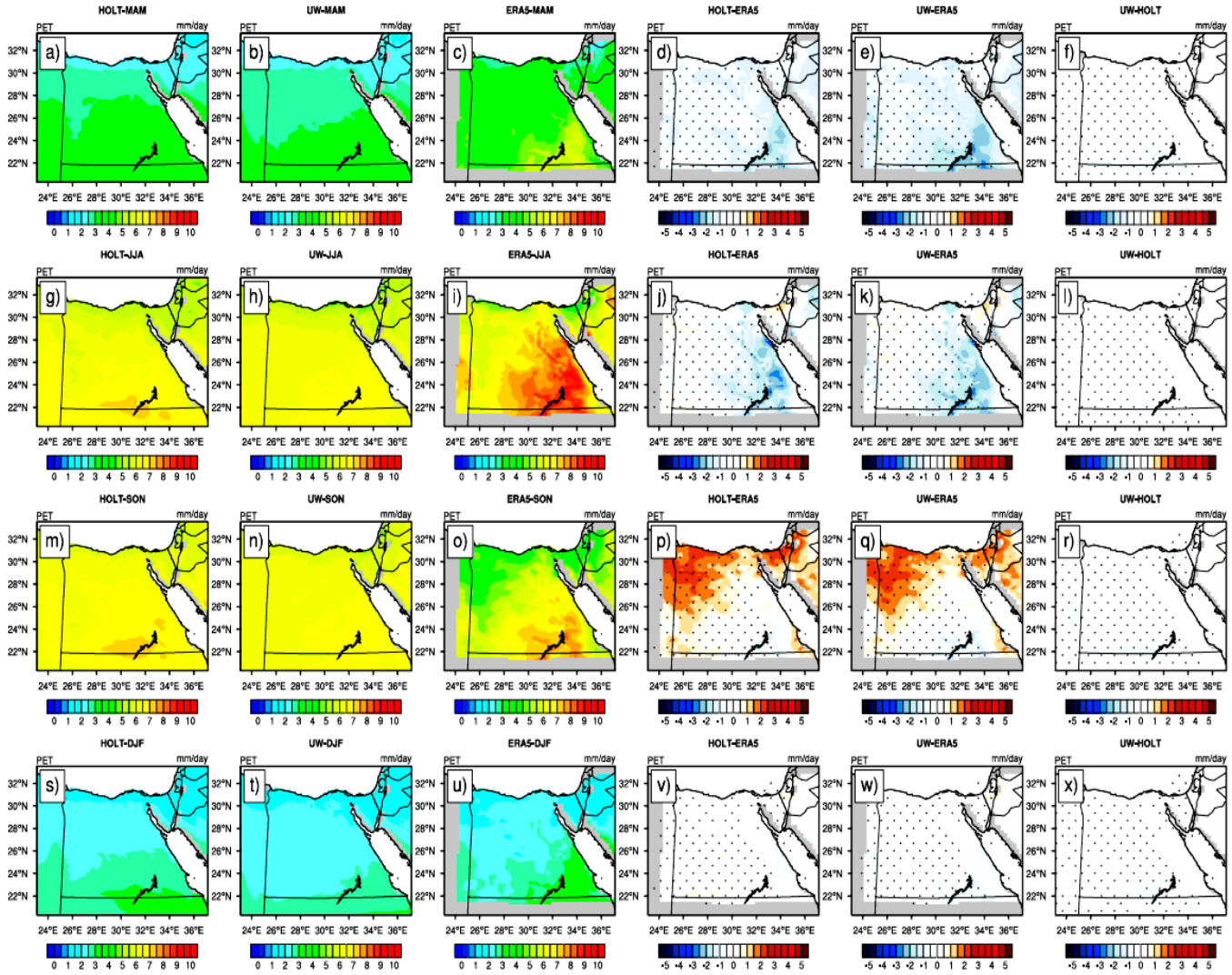

Figure 3. The figure shows the potential evapotranspiration over the period 1998–2017 (PET; in mm day^{-1}) for: MAM season in the first row (**a**–**f**); JJA in the second (**g**–**l**); SON in the third (**m**–**r**); and DJF in the fourth (**s**–**x**). For each row, HOLT is on the left, followed by UW; ERA5 is the third from left, HOLT minus ERA5, UW minus ERA5 and the difference between UW and HOLT. Significant difference/bias is indicated in black dots using student *t*-test with alpha equals to 5%.

3.2. Dependence of PET on RSDS and TMP

In Section 3.1, it was found that PET is insensitive to option of the dynamical downscaling or the boundary layer scheme despite of the noted changes of the TMP. Such point can be attributed to the fact that the RSDS is not affected by any of the two cases. Therefore, it was suggested that the RSDS is the main driver controlling the PET changes followed by the TMP. To confirm this point, a regional map of the Pearson correlation coefficient was plotted between the PET, RSDS and TMP for each case. The significant correlation was calculated using student *t*-test with alpha equals to 5%. Figure 4 shows the correlation between PET and TMP (Figure 4a), while the correlation between PET and RSDS is indicated in Figure 4b concerning the DIR simulation.

In Figure 4a, it can be observed that the correlation between PET and TMP exhibits a gradient differs with the region being examined. For instance in the region of 30–32° N, the gradient of PET–TMP correlation ranges between 0.9 and 0.94. While in the region of

22–28° N, the correlation ranges between 0.94 and 0.96. Regarding the PET–RSDS dependence, it can be seen that the correlation is between 0.96 and 0.98 (Figure 4c). For the NEST simulation, the PET–TMP dependence is quite different from the one observed in the DIR simulation because NEST is warmer than DIR in all seasons ([10]). This point can be indicated by noting that the correlation in this case ranges between 0.9 and 0.95 (Figure 4c). As for the RSDS, the situation is not quite different from the DIR simulation because RSDS does not change between the two simulations. Therefore, it can be observed that the correlation ranges from 0.96 to 0.98 similar to the DIR simulation (Figure 4d).

Concerning the case of the boundary layer parameterization, the PET–TMP correlation does not vary much between the boundary layer schemes (Figure 5a,c) compared to the case of the dynamical downscaling. For instance, the correlation (in the two simulations HOLT and UW) ranges between 0.9 and 0.96. This noted behavior can be attributed to two reasons: (1) the difference between DIR and NEST is larger than HOLT and UW and (2) regarding of TMP changes between HOLT and UW, RSDS is the main driver of PET changes followed by TMP. Regarding RSDS, there is only 1% difference between the correlations of the two simulations. For example for the HOLT simulation (Figure 5c), the correlation is between 0.96 and 0.98. On the other hand, the correlation ranges between 0.95 and 0.98 (Figure 5d) for the UW simulation.

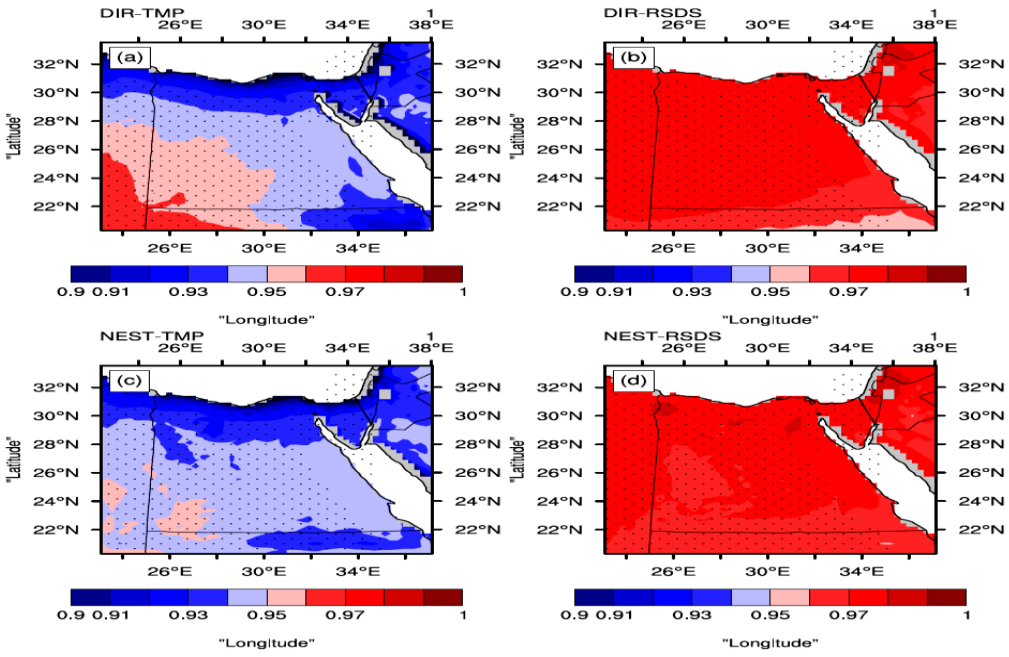

Figure 4. The figure shows the Pearson correlation coefficient for each grid point for: DIR ((**a**) for TMP), ((**b**) for RSDS); NEST ((**c**) for TMP) and ((**d**) for RSDS). Note that the range of 0.9 and 1 has been chosen after many trials to choose the appropiate range.

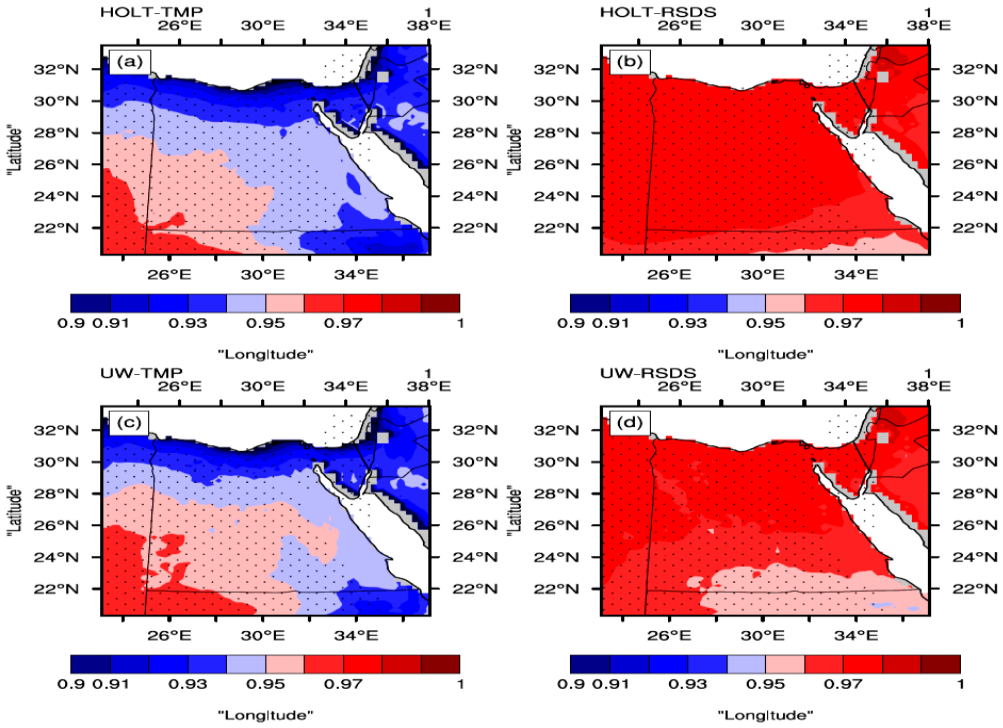

Figure 5. The figure shows the Pearson correlation coefficient for each grid point for: HOLT ((**a**) for TMP), ((**b**) for RSDS); UW ((**c**) for TMP) and ((**d**) for RSDS). Note that the range of 0.9 and 1 has been chosen after many trials to choose the appropiate range.

3.3. Climatological Annual Cycle of PET

To evaluate the simulated PET (on a point scale), the combination of DIR–UW (referred to as RegCM4) has been considered based on recommendation of [11]. The climatological annual cycle of the PET was evaluated with respect to ERA5 at locations of [3] except for Port-Said and Marsa-Matruh as discussed in Section 2.3. Preliminary analysis indicated that the simulated PET annual cycle can be categorized as: phase (Figure 6) and non-phase shift (Figure 7). This means that in the phase-shift, the simulated PET maximum value is either delayed or advanced with respect to the ERA5. On the other hand, the non-phase-shift considers consistency in the PET maximum value between RegCM4 and ERA5. Each phase comprises five stations. For instance, Figure 5 shows the annual cycle of the simulated PET (in comparison with the ERA5) for the locations: Alexandria, Arish, Giza, Ismaila and Siwa.

On the other hand, Figure 7 considers the comparison between the simulated PET and ERA5 for the locations: Asswan, Asyout, Dakhla, Kharga and Luxor. In Figure 6, it can be noted that the RegCM4 underestimates the PET (from month January to June), while it overestimates the PET during rest of months in Alexandria. Additionally, the RegCM4's peak lies in month August and ERA5's peak occurs in month June. The three locations (Arish, Giza, Ismaila, and Siwa) share a common feature regarding the RegCM4's behavior with respect to the ERA5. For instance in the aforementioned locations, the RegCM4 is close to the ERA5 from month January to May; while the RegCM4 overestimates the PET during rest of months. Similar to Alexandria, the RegCM4's peak occurs in month August while the ERA5's peak lies in month June. In Giza, the RegCM4's peak occurs in months July and August; while ERA5's peak occurs in months June and July.

From Figure 6, it be noted that the RegCM4 model has a limited ability to reproduce the climatological annual cycle of the simulated PET with the ERA5 for the coastal locations (Alexandria, Arish, Ismaila and Siwa) and near-coast location (Giza). In Figure 7, the situation is different because the RegCM4 is able to reproduce the simulated annual cycle

of the PET compared to the ERA5. For instance, both the RegCM4 and ERA5 show the PET's peak during the months June, July and August. Additionally, the RegCM4 underestimates the PET in the months of January till August, while the RegCM4 is close to the ERA5 during rest of months.

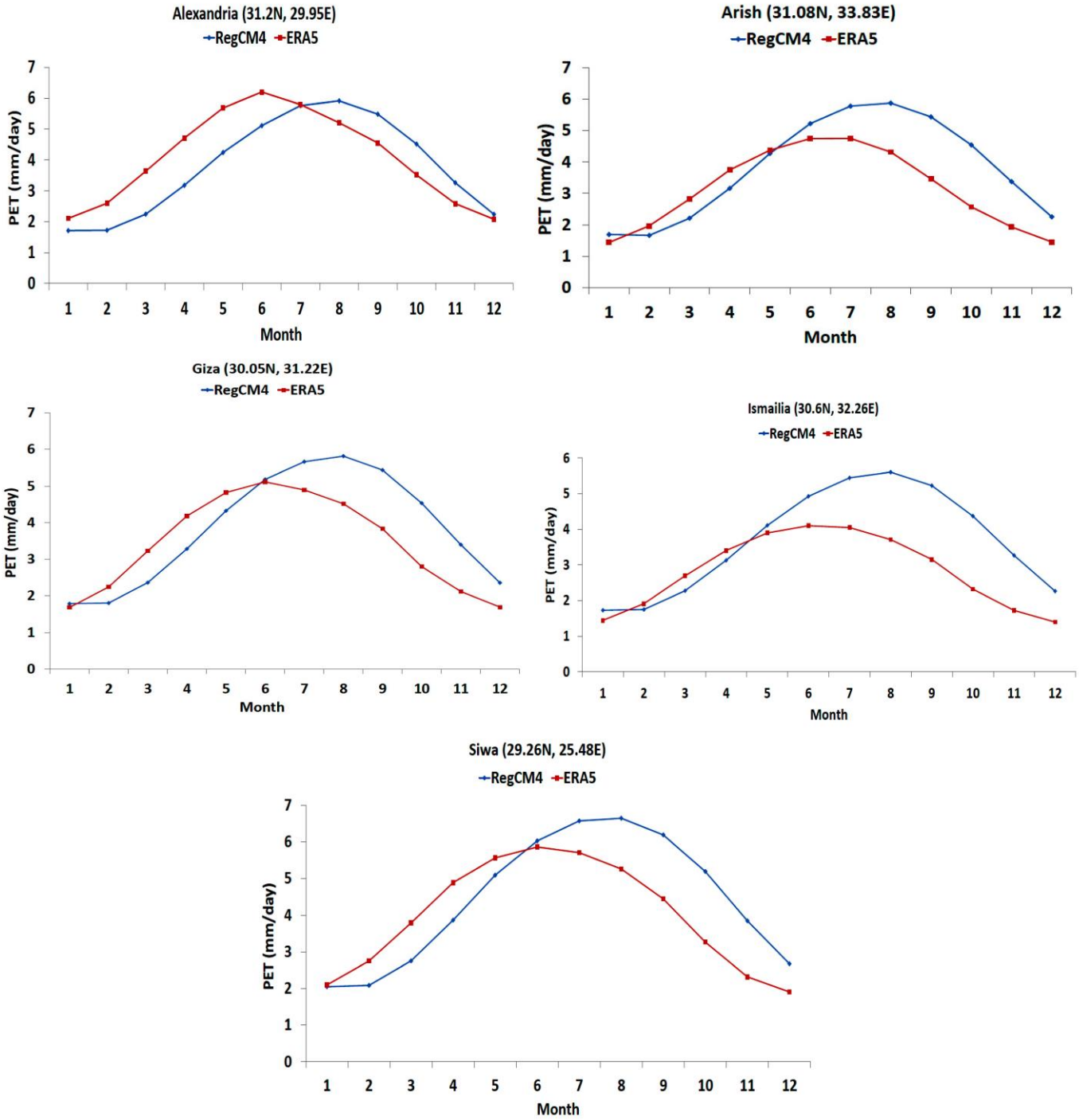

Figure 6. The figure shows the climatological annual cycle of the simulated PET with respect to the ERA5 for the locations: Alexandria, Arish, Giza, Ismaila and Siwa.

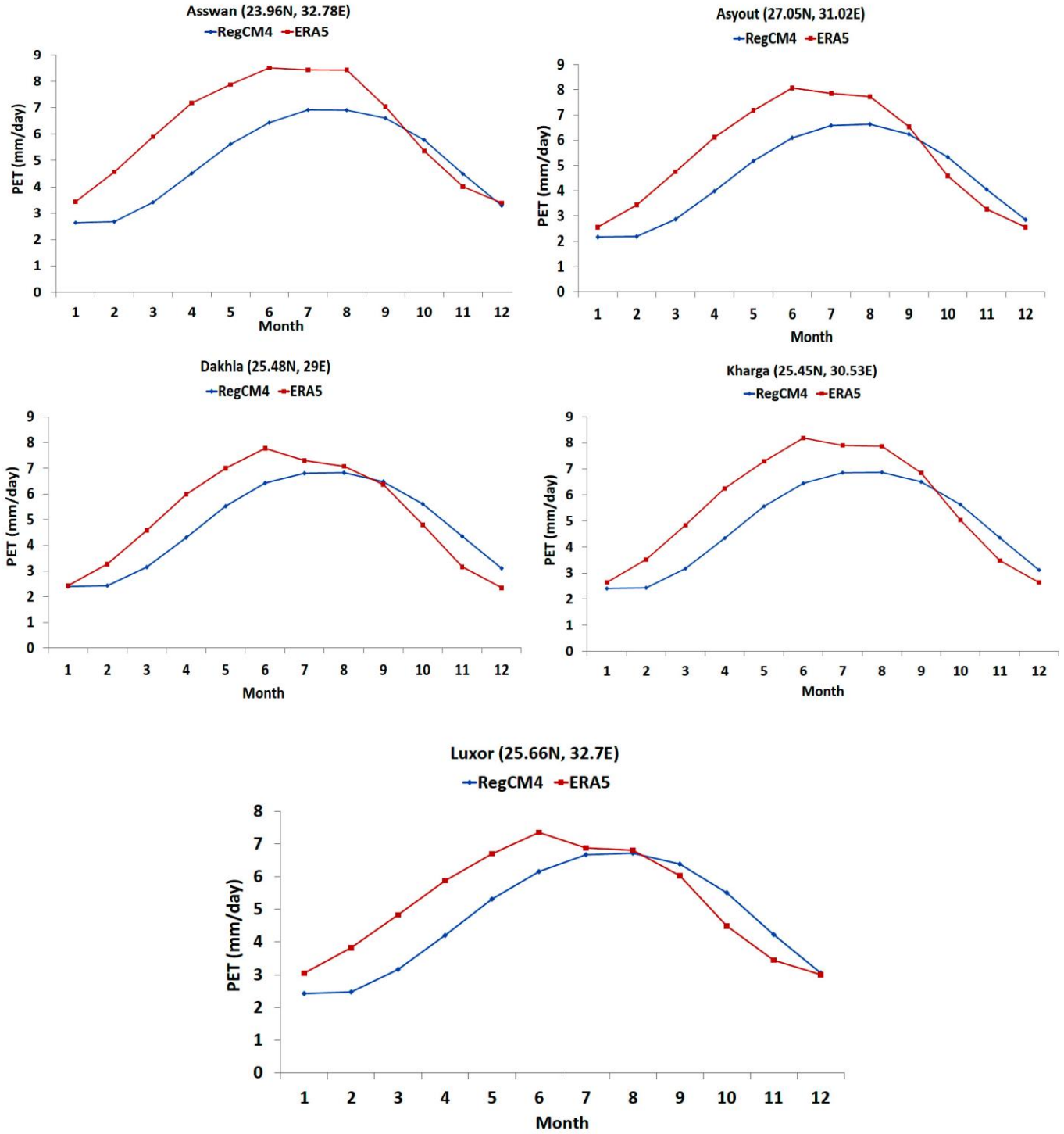

Figure 7. The figure shows the climatological annual cycle of the simulated PET with respect to the ERA5 for the locations: Asswan, Asyout, Dakhla, Kharga and Luxor.

4. Discussion and Conclusions

Accuracy of estimating the Potential evapotranspiration (PET) is a mandatory request for proper assessment of crop water needs as well as monitoring of agricultural and meteorological droughts. To achieve this accuracy, the authors of [2] recommended the PM equation to estimate the PET. However, the PM equation is data-intensive; which means that it requires many atmospheric variables not available spatially/temporary as reported by [21]. Therefore, there was an urgent need to possibly estimate the PET using a simple empirical method with a minimum number of meteorological inputs [3,4].

However, the original version of the empirical equation may not be suitable for estimating the PET causing over/underestimation with respect to observations of the PM. Therefore, local calibration (according to region of study) can give reasonable accuracy of estimating the PET.

Focusing on the HS equation (the alternative model following PM), the calibration has provided its efficiency in various regions across the globe such as: Egypt [4], Bulgaria [6], Sudan and South Sudan [21], West Texas [22] and Nigeria [23]. Additionally, accuracy of the calculated PET is not only affected by calibrating the empirical equation but also by the configuration of the regional climate model (e.g., RegCM4) used for this purpose. In fact, the authors of [9] used the RegCM4 model to conduct two experiments: (1) studying the influence of direct down-scaling of ERA-Interim reanalysis with different horizontal grid spacing and (2) making a comparison between direct down-scaling and two-way nesting using ERA-Interim of 1.5 degrees on the near daily average air temperature and total surface precipitation. They reported that the accuracy of the RegCM4 improved when direct down-scaling with fine resolution outperforms the coarse resolution. Furthermore, the direct downscaling outperforms the two-way nesting in simulating the mean air temperature and total surface precipitation.

In Egypt, a comparison has been conducted between the direct downscaling and one-way nesting investigating its influence on the daily mean air temperature [10]. In this study, the authors found that direct downscaling (DIR) outperforms the one-way nesting (NEST); such performance was indicated by a low bias of the direct downscaling compared to the one-way nesting (in which the RegCM4 bias has been amplified). Additionally, the accuracy of the RegCM4 has been examined by various schemes of the boundary layer [11]. In this study, the authors reported that the UW scheme is better than the HOLT in simulating the daily mean air temperature with respect to the ERA5. However, the influence of dynamical downscaling options or the role of the boundary layer schemes has not been examined for the PET of Egypt until the present day.

The present study addressed the influence of different options of dynamical downscaling and boundary layer schemes by conducting four simulations with 25 km horizontal grid spacing over the period 1997–2017. Also, the simulated PET was calculated using a calibrated version of the HS following [4]. The high−resolution global gridded PET product (hPET) was used as the benchmark for evaluating the simulated PET. The results of this study are summarized in the following points:

1. The simulated PET is insensitive to the choice of either the option of the dynamical downscaling or the boundary layer schemes despite of noted changes of the TMP reported in [10,11].
2. RSDS is the main driver of PET changes followed by the TMP. This noted behavior was indicated by a higher Pearson correlation coefficient (for each grid point) between PET and RSDS than between PET and TMP for each case (see Section 3.2).
3. On a point-scale, the simulated climatological annual cycle of the PET has been categorized as: phase and non-phase shift. Additionally, the noted over/underestimated PET varies with location and month.

In conclusion, the RegCM4 can be used to develop a PET map of Egypt using the DIR-UW configuration. This finding not only aids policy makers in assessing the daily water requirements of crops, which is crucial for daily forecasts, especially in regions with limited data, but also holds potential for projecting future water needs under varying warming scenarios. Such insights provide a vital resource for strategic decision-making in agricultural and water resource management, offering a bridge between scientific advancements and actionable policies.

It is worth mentioning that the present study did not consider the influence of aerosols affecting the RSDS budget and eventually the simulated PET. Also, long term in-situ observations were not available during time of experiment. Instead, we used hPET to evaluate the RegCM4 performance on a point scale. Additionally, bias-correction techniques

(e.g., [14]) have not been applied to correct the RegCM4 output of each season. Finally, the present study relies on using one regional climate model (RCM) as the simulated TMP and RSDS are affected by the uncertainty associated with the RCM and eventually the PET. In a future study the following points will be addressed:

1. Considering the influence of aerosols to address the notes changes of RSDS, TMP and PET.
2. Revising the work of [3] by: calculating the simulated PET following [4] and considering the DIR downscaling option and UW as the boundary layer scheme using hPET product as the ground truth of observation following [4].
3. Studying the sensitivity of the simulated PET to different lateral boundary conditions (adopted from the General Circulation Models participated in the Fifth Coupled Model Intercomparison Project—CMIP5; [24]) by examining the simulated RSDS and TMP following [6,15,25].

Supplementary Materials: The following supporting information can be downloaded at: www.mdpi.com/xxx/s1, Figure S1: The figure shows a methodological flowchart summarizing the steps of the present study.

Author Contributions: Conceptualization, S.A.A.; methodology, S.A.A.; software, S.A.A.; validation, S.A.A.; formal analysis, S.A.A. and A.S.; investigation, S.A.A. and A.S.; resources, S.A.A.; data curation, S.A.A.; writing—original draft preparation, S.A.A. and A.S.; writing—review and editing, S.A.A. and A.S.; visualization, S.A.A.; supervision, S.A.A. and A.S.; project administration, S.A.A. All authors have read and agreed to the published version of the manuscript.

Funding: This research received no external funding.

Institutional Review Board Statement: Not applicable.

Informed Consent Statement: Not applicable.

Data Availability Statement: Not applicable.

Acknowledgments: Egyptian Meteorological Authority (EMA) is acknowledged for providing the computational power to conduct the model simulations. Hourly potential evapotranspiration (hPET) was retrieved from the web link https://data.bris.ac.uk/data/dataset/qb8ujazzda0s2aykkv0oq0ctp. However, the monthly mean can be acquired from the authors upon request (accessed on 18 October 2022).

Conflicts of Interest: The authors declare no conflict of interest.

References

1. IPCC. *Climate Change 2007: Synthesis Report*; Technical report; IPCC: Geneva, Switzerland, 2007.
2. Allen, G.R.; Pereira, S.L.; Raes, D.; Smith, M. *Crop Evapotranspiration: Guidelines for Computing Crop Water Requirements*; Report 56; Food and Agricultural Organization of the United Nations (FAO): Rome, Italy, 1998; 300p.
3. Anwar, S.A.; Salah, Z.; Khaled, W.; Zakey, A.S. Projecting the Potential Evapotranspiration in Egypt Using a High-Resolution Regional Climate Model (RegCM4). *Environ. Sci. Proc.* **2022**, *19*, 43. https://doi.org/10.3390/ecas2022-12841.
4. Anwar, S.A.; Lazić, I. Estimating the Potential Evapotranspiration of Egypt Using a Regional Climate Model and a High-Resolution Reanalysis Dataset. *Environ. Sci. Proc*. **2023**, *25*, 29. https://doi.org/10.3390/ECWS-7-14253.
5. Hargreaves, G.L.; Allen, R.G. History and evaluation of Hargreaves evapotranspiration equation. *J. Irrigat. Drain. Eng*. **2003**, *129*, 53–63.
6. Anwar, S.A.; Malcheva, K.; Srivastava, A. Estimating the potential evapotranspiration of Bulgaria using a high-resolution regional climate model. *Theor. Appl. Climatol.* **2023**, *152*, 1175–1188. https://doi.org/10.1007/s00704-023-04438-9.
7. Giorgi, F.; Coppola, E.; Solmon, F.; Mariotti, L.; Sylla, M.B.; Bi, X.; Elguindi, N.; Diro, G.T.; Nair, V.; Giuliani, G.; et al. BrankovicRegCM4: Model description and preliminary tests over multiple CORDEX domains. *Clim. Res.* **2012**, *52*, 7–29.
8. Chen, L.; Huang, G.; Wang, X. Projected changes in temperature, precipitation, and their extremes over China through the RegCM. *Clim. Dyn*. **2019**, *53*, 5859–5880. https://doi.org/10.1007/s00382-019-04899-7.
9. Xu, X.; Huang, A.; Huang, Q.; Zhang, Y.; Wu, Y.; Gu, C.; Cai, S.; Zhu, X. Impacts of horizontal resolution of the lateral boundary conditions and downscaling method on the performance of RegCM4.6 in simulating the surface climate over central-eastern China. *Earth Space Sci.* 2022, 9, e2022EA002433. https://doi.org/10.1029/2022EA002433.
10. Anwar, S.A. Influence of Direct-Downscaling and One-Way Nesting on Daily Mean Air Temperature of Egypt Using the RegCM4. *J. Biomed. Res. Environ. Sci.* **2023**, *4*, 338-347. https://doi.org/10.37871/jbres1681.

11. Anwar, S.A.; Mostafa, S.M. On the Sensitivity of the Daily Mean Air Temperature of Egypt to Boundary Layer Schemes Using a High-Resolution Regional Climate Model (RegCM4). *J. Biomed. Res. Environ. Sci.* **2023**, *4*, 474–484. https://doi.org/10.37871/jbres1700.
12. Grenier, H.; Bretherton, C.S. A moist PBL parameterization for large scale models and its application to subtropical cloud topped marine boundary layers. *Mon. Weather Rev.* **2001**, *129*, 357–377.
13. Holtslag, A.A.M.; Boville, B.A. Local versus nonlocal boundary layer diffusion in a global model. *J. Clim.* **1993**, *6*, 1825–1842.
14. Mostafa, S.M.; Anwar, S.A.; Zakey, A.S.; Wahab, M.M.A. Bias-correcting the maximum and minimum air temperatures of Egypt using a high-resolution Regional Climate Model (RegCM4). *Eng. Proc.* **2023**, *31*, 73. https://doi.org/10.3390/ASEC2022-13852.
15. Anwar, S.A.; Mamadou, O.; Diallo, I.; Sylla, M.B. On the influence of vegetation cover changes and vegetation-runoff systems on the simulated summer potential evapotranspiration of tropical Africa using RegCM4. *Earth Syst. Environ.* **2021**, *5*, 883–897. https://doi.org/10.1007/s41748-021-00252-3.
16. Anwar, S.A.; Diallo, I. A RCM investigation of the influence of vegetation status and runoff scheme on the summer Gross Primary Production of Tropical Africa. *Theor. Appl. Climatol.* **2021**, *145*, 1407–1420. https://doi.org/10.1007/s00704-021-03667-0.
17. Dee, D.P.; Uppala, S.M.; Simmons, A.J.; Berrisford, P.; Poli, P.; Kobayashi, S.; Andrae, U.; Balmaseda, M.A.; Balsamo, G.; Bauer, P.; et al. The ERA-Interim reanalysis: Configuration and performance of the data assimilation system. *Q. J. R. Meteorol. Soc.* **2011**, *137*, 553–597.
18. Singer, M.; Asfaw, D.; Rosolem, R.; Cuthbert, M.O.; Miralles, D.G.; MacLeod, D.; Michaelides, K. Hourly potential evapotranspiration (hPET) at 0.1degs grid resolution for the global land surface from 1981-present. *Sci. Data* **2021**, *8*, 224. https://doi.org/10.1038/s41597-021-01003-9.
19. Muñoz-Sabater, J.; Dutra, E.; Agustí-Panareda, A.; Albergel, C.; Arduini, G.; Balsamo, G.; Boussetta, S.; Choulga, M.; Harrigan, S.; Hersbach, H.; et al. ERA5-Land: A state-of-the-art global reanalysis dataset for land applications. *Earth Syst. Sci. Data* **2021**, *13*, 4349–4383. https://doi.org/10.5194/essd-13-4349-2021.
20. Harris, I.; Osborn, T.J.; Jones, P.; Lister, D. Version 4 of the CRU TS monthly high-resolution gridded multivariate climate dataset. *Sci. Data* **2020**, *7*, 109. https://doi.org/10.1038/s41597-020-0453-3.
21. Elagib, N.A.; Musa, A.A. Correcting Hargreaves-Samani formula using geographical coordinates and rainfall over different timescales. *Hydrol. Process.* **2023**, *37*, e14790. https://doi.org/10.1002/hyp.14790.
22. Awal, R.; Rahman, A.; Fares, A.; Habibi, H. Calibration and Evaluation of Empirical Methods to Estimate Reference Crop Evapotranspiration in West Texas. *Water* **2022**, *14*, 3032. https://doi.org/10.3390/w14193032.
23. Ogunrinde, A.T.; Emmanuel, I.; Enaboifo, M.A.; Ajayi, T.A.; Pham, Q.B. Spatio-temporal calibration of Hargreaves–Samani modelin the Northern Region of Nigeria. *Theor. Appl. Climatol.* **2022**, *147*, 1213–1228. https://doi.org/10.1007/s00704-021-03897-2.
24. Taylor, K.E.; Stoufer, R.J.; Meehl, G.A. An overview of CMIP5 and the experiment design. *Bull. Am. Meteorol. Soc.* **2012**, *90*, 485–498. https://doi.org/10.1175/BAMS-D-11-00094.1.
25. Anwar, S.A.; Diallo, I. Modelling the Tropical African Climate using a state-of-the-art coupled regional climate-vegetation model. *Clim. Dyn.* **2022**, *58*, 97–113.